



Exosome-based cancer vaccine for prevention of lung cancer

Shuhan Meng^{1,2}, Aaron G. Whitt^{1,2}, Bryce F. Stamp^{3,4}, John W. Eaton^{1,2,5}, Chi Li^{1,2,5}, Kavitha Yaddanapudi^{3,4,6}

¹Department of Pharmacology and Toxicology, University of Louisville, Louisville, KY, USA; ²Experimental Therapeutics Program, Brown Cancer Center, University of Louisville, Louisville, KY, USA; ³Department of Surgery, Division of Immunotherapy, University of Louisville, Louisville, KY, USA; ⁴Immuno-Oncology Program, Brown Cancer Center, University of Louisville, Louisville, KY, USA; ⁵Department of Medicine, University of Louisville, Louisville, KY, USA; ⁶Department of Microbiology and Immunology, University of Louisville, Louisville, KY, USA

Contributions: (I) Conception and design: K Yaddanapudi, C Li, JW Eaton; (II) Administrative support: K Yaddanapudi, C Li, JW Eaton; (III) Provision of study materials or patients: S Meng, AG Whitt, BF Stamp; (IV) Collection and assembly of data S Meng, AG Whitt, BF Stamp, C Li, K Yaddanapudi; (V) Data analysis and interpretation: K Yaddanapudi, C Li, JW Eaton; (VI) Manuscript writing: All authors; (VII) Final approval of manuscript: All authors.

Correspondence to: Chi Li. Department of Pharmacology and Toxicology, University of Louisville, Louisville, KY, USA. Email: chi.li@louisville.edu; Kavitha Yaddanapudi. Department of Surgery, Division of Immunotherapy, University of Louisville, Louisville, KY, USA. Email: kavitha.yaddanapudi@louisville.edu.

Background: Our earlier work has shown that a unique stem cell-based vaccine that comprises of murine embryonic stem cells (ESCs) and murine fibroblasts expressing the immunostimulant granulocyte-macrophage colony stimulating factor (GM-CSF) successfully protects mice from the outgrowth of an implantable form of murine lung cancer. The use of live ESCs raises the potential risks of inducing teratomas and autoimmunity. We have attempted to improve the safety and utility of this prophylactic vaccine by employing exosomes derived from murine ESCs engineered to produce GM-CSF (ES-exo/GM-CSF vaccine).

Methods: We have previously reported that ES-exo/GM-CSF immunization does protect mice from the outgrowth of an implantable form of murine lung cancer. Here, we have investigated the cancer prevention efficacy of ES-exo/GM-CSF vaccine in an experimental metastasis model of murine lung cancer, in which Lewis lung carcinoma (LLC) cells were administered into female C57BL/6 mice (8 weeks of age) through tail vein injection and subsequently LLC tumors were established in lungs.

Results: Our objective is to test the anti-cancer efficacy of ES-exo/GM-CSF vaccine in a mouse model of metastatic lung cancer. Our studies indicate that vaccination of mice with ES-exo/GM-CSF vaccine inhibited the growth of metastatic lung tumors. ES-exo/GM-CSF vaccination reduced lung tumor burden from 1.86% in non-vaccinated, LLC-challenged mice to 0.036% in corresponding vaccinated mice. Importantly, control exosomes without GM-CSF failed to provide protection against metastasized pulmonary tumors. The efficacy of ES-exo/GM-CSF vaccination was associated with a decrease in the frequencies of tumor-infiltrating immunosuppressive immune cells, including T regulatory cells, myeloid derived suppressor cells (MDSCs) and tumor-associated macrophages, as well as an increase in effector cytokine production from intra-tumoral CD8⁺ T cells.

Conclusions: Overall, our research provides a novel strategy for developing a cell-free prophylactic vaccine against lung tumors.

Keywords: Exosome; vaccine; lung cancer; metastasis

Received: 16 September 2022; Accepted: 21 December 2022; Published online: 09 January 2023.

doi: 10.21037/sci-2022-030

View this article at: <https://dx.doi.org/10.21037/sci-2022-030>

Introduction

A prophylactic cancer vaccine is a promising approach to reduce pulmonary malignancy. The majority of cancer vaccines under development usually need robust adjuvants to enhance the immune response because most of the tumor antigens targeted in vaccines are identical to “self” antigens (1). However, the efficacy of a lung cancer vaccine will be markedly increased if the vaccine targets multiple “non-self” antigens presented only by lung tumors (2). Emerging evidence has demonstrated that tumor cells and embryonic stem cells (ESCs) share common antigens that are considered as “non-self” antigens, because they are not expressed in normal adult tissues (3,4). Based on the antigenic similarity between malignant cells and ESCs, researchers have developed a prophylactic lung cancer vaccine composed of irradiated, intact murine ESCs and murine fibroblasts expressing the immunostimulatory adjuvant granulocyte-macrophage colony stimulating factor (GM-CSF) (5). In support of cancer prevention capability of ESCs, two recent studies have demonstrated that irradiated, induced pluripotent stem cells (iPSCs) along with the adjuvant CpG function as a tumor vaccine to elicit an anti-tumor response against transplanted breast cancer, mesothelioma, melanoma and pancreatic cancer (6,7).

Despite the promise of ESC- or iPSC-based vaccine to evoke anti-lung cancer immune responses, such a vaccine has two obvious challenges to overcome for human application. First, the administration of intact ESCs or iPSCs, albeit irradiated, raises the risk of embryoma/teratoma formation and autoimmunity caused by inherent tumorigenic and immunogenic properties of ESCs or iPSCs (8). Furthermore, it is unnecessarily complicated to use fibroblasts as a source for the adjuvant GM-CSF. To overcome these hurdles, we have developed an alternative prophylactic vaccine comprised of exosomes from murine ESCs engineered to produce GM-CSF (ESC-exo/GM-CSF). This self-contained, relatively stable exosome-based vaccine significantly slowed or blocked the outgrowth of subcutaneously implanted lung tumors (9).

As small membrane vesicles released from various cell types, exosomes have been reported to function as essential mediators of intercellular communication and play a basic role in many (patho)physiological processes, including tumorigenesis (10). Exosomes have been engineered to enhance immunoresponses against cancer as therapeutics for treatment or vaccines for prevention (11,12). As cell-

free agents, exosomes are advantageous over cell-based therapeutic therapies in several aspects, due to their superior bio-availability, excellent bio-stability, and lower expenses.

Metastasis results from the tumor cells on primary sites migrating to distant organs. The process of metastasis includes cancer cell proliferation, angiogenesis, cell adhesion, migration and invasion into the surrounding tissue (13,14). The prognosis of cancer patients decreases dramatically once metastasis happens (15,16). Despite ongoing progress in diagnosis and patient care, metastasis is still the principal cause of mortality from neoplastic diseases. Lung metastasis occurs when malignant cells originating in another organ of the body migrate to and establish in the lung. Chemotherapy is the most commonly used therapy for lung metastasis with modest efficacy (17). Therefore, if malignant cells metastasizing to the lung could be recognized by the immune system and eliminated before their establishment and growth in the lung, it would have promising application in clinics.

Mouse models of orthotopic lung cancer have been effective tools for investigating and possibly treating lung cancer by recapitulating the process of pulmonary malignancy (18). So far, several orthotopic lung cancer mouse models have been established and they primarily differ in how lung cancer cells are administered, including intrathoracic injection, transbronchial implantation and tail vein injection (19). For lung cancer cells injected into the tail vein, a small number of cells are able to reach the lung through blood circulation, where tumors are established (20-22). This experimental strategy is also called “experimental metastasis”, which is often used to investigate the potential of intravenously injected lung tumor cells to seed, extravasate and develop into metastases in the lung. In this study, our objective is to investigate the efficacy of ES-exo/GM-CSF in an experimental metastasis model. We show that ES-exo/GM-CSF vaccination effectively prevents the outgrowth of metastasized lung tumors in mice. Notably, the anti-tumor efficacy of this vaccination strategy is associated with reduced tumor-promoting immune cells and increased tumor-suppressing immune cells in lung metastases. Overall, our research provides a strategy for developing a cell-free preventative vaccine against metastasized lung tumors. We present the following article in accordance with the ARRIVE reporting checklist (available at <https://sci.amegroups.com/article/view/10.21037/sci-2022-030/rc>).

Methods

Mice

Female C57BL/6 mice (8 weeks of age) were purchased from Jackson Laboratory (Bar Harbor, ME) and housed at the University of Louisville pathogen-free Research Resources Facilities (RRF) located at the basement of Clinical Translational Research Building (CTRB) under standard conditions. Mice were in good health conditions free of pathogens.

Randomization

Female mice were randomly allocated to control and experimental groups.

Confounders: Confounders were not controlled.

Blinding

Blinding was implemented during the outcome analysis (tumor measurements) and data analysis (calculations of tumor volume). Blinding was not implemented during the allocation of control and treatment groups and during the treatment of mice with vaccine and vehicle.

Inclusion and exclusion criteria

No Criteria was set up to include or exclude animals from the control and treatment groups.

Housing and husbandry conditions

Mice were bred and housed in a pathogen-free barrier animal facility and maintained on a standard 12-hour light/12-hour dark cycle. Throughout the proposed studies, the mice had full access to water and food.

Veterinary care of animals

Veterinary care and maintenance were provided by the University of Louisville CTRB Barrier Animal Facility which provides housing and procedure assistance for mouse studies via full technical and veterinary support. The facility is staffed 7 days per week, has AAALAC (American Association for Accreditation of Laboratory Animal Care) Accreditation, and OPRR IACUC (Office for Protection from Research Risks, Institutional Animal Care and Use Committee) Assurance.

Procedures for minimizing discomfort, distress, pain, and injury

All mice were monitored closely for signs of discomfort, difficulty in breathing or restriction in normal activities

(e.g., eating, drinking or ambulation) due to tumor bulk. Other potential adverse effects from tumor growth could be related to pain or distress from the direct and systemic side effects of tumor growth that would be displayed by specific behavioral changes and clinical signs. The recognition of pain and distress in mice were accomplished by examining the mice frequently for specific changes in general behavior, appearance and physiology. Accordingly, mice were monitored once daily for the following: excessive licking, guarding of limbs, self-mutilation, increased vocalization, reduced appetite or drinking, un-groomed appearance, piloerection, abnormal stance, increased movement, hunched posture, eyelids partly closed, pupils dilated, nasal discharge, shallow breathing and grunting. In the event of any signs of pain and distress or any adverse effects due to tumor burden, the mice were promptly euthanized by CO₂ asphyxiation.

Ethics statement

Mice were handled in accordance with the AAALAC guidelines and the “Guide for the Care and Use of Laboratory Animals” (Institute of Laboratory Animal Resources, National Research Council, National Academy Press, 1996). The mouse study was approved by the IACUC of the University of Louisville (protocol number: 18301).

Cell culture

LLC cells were acquired from ATCC (Manassas, VA, USA) and cultured in Dulbecco's Modified Eagle's Medium (Mediatech; Manassas, VA, USA) supplemented with 10% fetal bovine serum (Gemini; Broderick, CA, USA), 100 units/mL penicillin (Mediatech), and 100 µg/mL streptomycin (Mediatech). The cells were cultured in a 5% CO₂ humidified incubator at 37 °C, The cells were passaged at 1:5–1:10 dilutions and continuously cultured no longer than 3 weeks.

RNA-sequencing

Total RNA in ES-D3 cells and Lewis lung carcinoma (LLC) cells was isolated using a RNeasy kit (Qiagen; Germantown, MD, USA). mRNA libraries were prepared using a TruSeq Stranded mRNA Library Prep Kit (Illumina; San Diego, CA, USA) according the manufacture's protocol. RNA sequencing were performed on a NextSeq 500 system using a NextSeq 500/550 1x75 cycle High Output Kit v2.5

(Illumina). RNA-sequencing data were analyzed using the Tuxedo suite (Illumina).

ELISA

The amounts of GM-CSF in isolated exosomes were determined using an ELISA kit for murine GM-CSF (88733422; Thermo Fisher, Waltham, MA, USA). GM-CSF levels in the exosomes were measured following manufacturer's instructions with some modifications. Specifically, exosomes (0.6 μg) were incubated in phosphate buffered saline (PBS) alone or PBS + 0.05% Tween-20 (100 μL) at room temperature for 30 minutes. Treated samples were added to a capture antibody-coated ELISA plate. Samples treated with PBS alone were washed with PBS and samples treated with PBS + 0.05% Tween-20 were washed with PBS + 0.05% Tween-20. After incubation with detection antibody and Avidin-HRP, the concentrations of GM-CSF were determined by measuring the absorbance at 450 nM on a microplate reader (PowerWave XS; BioTek, Winooski, VT).

Vaccination and tumor challenge

Exosomes from ES-D3 cells were acquired as described before (9). Female C57BL/6 mice (8 weeks of age) were immunized twice (days 0 and 7) with vehicle only (PBS), 225 μg exosomes isolated from ES-D3 cells expressing the empty vector (ES-Exo) or 225 μg exosomes isolated from ES-D3 cells stably-expressing GM-CSF (ES-Exo/GM-CSF) as described in our previous study (9). Exosomes were injected subcutaneously (s.c.) in the right flank of mice. Following vaccination, mice were challenged with LLC cells (0.15×10^6) by tail vein injection on day 14. Immunology analysis of splenocytes and tumor-infiltrating lymphocytes (TILs) were carried out 5 weeks following LLC cell challenge. Lung tumorigenesis was examined at 6 weeks (10 mice in each group, total 30 mice, 5 mice/cage) or 7 weeks (11 mice in control group, 9 mice in ES-exo group and 10 mice in ES-exo/GM-CSF group, total 30 mice, 5 mice/cage) after LLC cell injection. With 10 mice in each group ($n_1 = 10$ and $n_2 = 10$), an effect size of 2.2 fold could be detected, using a one-tailed *t* test ($\alpha = 0.05$, power of 80%) and assuming common standard deviation. One mouse in ES-exo (7-week) group became limp after LLC injection, due to a leg injury. The mouse was euthanized following the instruction of veterinary staff members and IACUC protocol. End points for experiments with mice were selected in accordance with institutional-approved

criteria. All tumor cell lines used in the *in vivo* experiments were routinely tested for mycoplasma contamination using Mycoalert plus mycoplasma detection kit (Lonza).

Histological analysis of lung tissues

Lung tissue sections were prepared as previously described with some modifications (23). Briefly, lung tissues were fixed in 10% neutral phosphate buffered formalin for 24 hours at room temperature. After paraffin processing (TEK VIP; Sakura Finetek; Torrance, CA, USA) and embedding (EG1160; Leica Biosystems; Buffalo Grove, IL, USA), paraffin microtomy (RM2135; Leica Biosystems) was performed at 5 microns thickness of slide for each section. Three sections were processed with 50 microns between each. For each biopsy core, three consecutive sections are placed on 3 slides (total of 9 sections per lung tissue) to assure detection of tumorigenesis in a whole lung. Slides of sections were deparaffinized and rehydrated in xylene, ethanol and deionized water. Slides were stained in hematoxylin (95057-844; VWR; Radnor, PA, USA). After rinsing with deionized water, the slides were stained by eosin (HT110232; Thermo Fisher) and dehydrated in ethanol and xylene. Coverslips were mounted on slides by xylene-based permountTM mounting medium (SP15-500; Thermo Fisher). Finally, the slides were dried overnight in a chemical hood. The slides were scanned by Aperio Imagescope (Leica Biosystems) and analyzed with the software (version 12.3.3).

Antibodies

Antibodies used for evaluating splenocytes and TILs were: anti-CD3 mAb (clone 17A2, 100222); anti-CD4 mAb (clone GK1.5; 100406); anti-CD8 mAb (clone 53-6.7; 100712); anti-CD11b mAb (clone M1/70; 101228); anti-Ly6C mAb (clone HK1.4; 128006); anti-Ly6G mAb (clone 1A8; 127608); anti-CD16/CD32 mAb (clone 2.4G2; 101320) from Biolegend (San Diego; CA, USA), anti-CD44 mAb (clone IM7; 17-0441-82); anti-CD25 mAb (clone PC61.5; 45-0251-82) from (Thermo Fisher), anti-CD62L mAb (clone MEL-14; 553152; BD Biosciences; San Jose, CA, USA).

Analysis of immune cells in the spleen

Five weeks following tail vein injection of LLC cells (0.15×10^6) into female C57BL/6 mice, spleens were resected and splenocytes were acquired. Single splenocyte suspensions were stained with the indicated antibodies for 30 minutes

after blocking with CD16/CD32 antibody for 15 minutes at 4 °C. After washing, cell surface and intracellularly stained cells were analyzed on a FACSCalibur (Becton Dickinson; Franklin Lakes, NJ) and results were analyzed using FlowJo software (TreeStar, Inc., Ashland, OR).

Analysis of tumor-infiltrating immune cells

Vaccinated and control mice with LLC tumors metastasized to lungs were euthanized 35 days after tumor challenge. Lungs were resected and metastasized LLC tumors were dissected and chopped into small pieces before incubation with a mixture of enzymes dissolved in HBSS, including collagenase type IV (400 U/mL; C9891; Sigma-Aldrich; St. Louis, MO, USA), hyaluronidase (0.025 mg/mL; H6254; Sigma-Aldrich) and DNase I (0.01 mg/mL; D5025; Sigma-Aldrich) for 30 minutes at 37 °C with occasional shaking. The resultant cells were washed and passed through a Ficoll gradient (17144002; GE Healthcare; Chicago, IL, USA) to eliminate dead cells. TILs were then analyzed by flow cytometry for the expression of markers for different immune cells. Anti-CD45 antibody was used to selectively exclude CD45⁻ tumor cells from analysis so that only CD45⁺ immune cells were evaluated. The same number of cells (based on side-scatter and forward-scatter analyses) was acquired in all samples. Respective antibodies specific for the markers were used to quantitate the abundance of different immune cell types. T regulatory cells (T_{regs}; Foxp3⁺) were analyzed using the anti-mouse Foxp3 staining kit (00-5523-00; Thermo Fisher).

Intracellular cytokine staining

To evaluate TNF- α and IFN- γ production, TILs were harvested and restimulated for 6 hours with the LLC lysate (50 μ g/mL) in the presence of GolgiplugTM (555029; BD Biosciences) at a concentration of 1 μ l/mL of culture medium. After restimulation, cells were harvested, Fc receptors were blocked using anti-CD16/CD32 antibodies, and cells were stained for surface expression of CD8 and intracellular expression of cytokines using Cytofix/Cytoperm kit (555029; BD Biosciences) according to the manufacturer's instructions and analyzed by flow cytometry.

Statistical analysis

The statistical analysis was conducted using StatView version 5.0.1 software (Windows version; SAS Institute, Cary, NC)

or GraphPad Prism 5.0 software (GraphPad Prism Software, Inc., La Jolla, CA, USA). Two-group comparisons between control and test samples (groups compared are indicated in the respective figures) were performed using Unpaired Student's *t* tests. Multiple data comparisons were derived by one-way ANOVA followed by Tukey's post-hoc test.

Results

ESCs and lung tumor cells share expression of tumor-associated genes

Emerging evidence indicates that cancer cells express certain embryonic antigens (i.e. carcinoembryonic antigens), which is also known as "retrogenetic expression" (3,4). To identify tumor-associated genes that are also expressed in ESCs, we evaluated gene expression profiles of the murine ESC cell line ES-D3 and the murine lung cancer cell line LLC by a RNA-sequencing approach (Figure 1). We profiled expression of a curated selection of 123 tumor-associated genes as described in (6). It was found that the majority of tumor-associated genes were also highly expressed in ES-D3 cells. Overall, these data suggest that shared expression of tumor-associated genes between ESCs and lung cancer cells can evoke immunity against pulmonary malignancy.

Evaluation of exosomes from ES-D3 cells expressing GM-CSF

In our earlier studies (9), immunostimulatory protein GM-CSF was stably expressed in ES-D3 cells by transfection. We reasoned that exosomes from ES-D3 cells expressing GM-CSF could also possess biological activities to regulate immune responses and prevent tumor growth. Towards this goal, exosomes from ES-D3 cells stably expressing GM-CSF or its empty vector were isolated after step-wise centrifugation and evaluated by transmission electron microscopy (Figure 2A). The high GM-CSF expression in ES-D3 cells had minimal impact on production levels of exosomes (Figure S1). Isolated exosomes were comprised of vesicles with sizes ranging from 30 to 100 nM, which is in agreement with previous reported sizes of exosomes from other sources (24). Purity of exosomal material was validated by the presence of exosomal markers Alix, annexin V and CD81 as well as the absence of markers of other subcellular compartments, including the endoplasmic reticulum marker calnexin, the mitochondrial markers cytochrome c and COX IV-subunit IV, and the cytosolic marker GAPDH

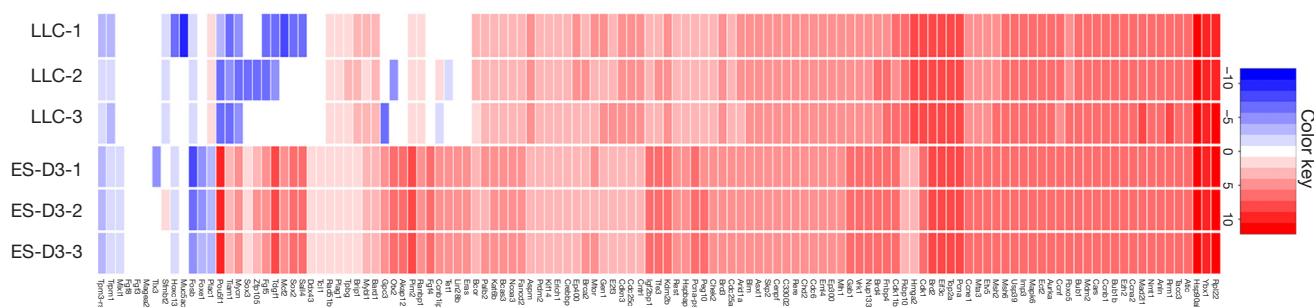


Figure 1 Murine ES cells and LLC cells share expression of tumor-associated genes. Heatmap analysis of RNA-sequencing data showing the expression of 123 tumor-associated genes in both ES-D3 cells and LLC cells (in triplicate). Red: high expression; Blue: low expression; White: equal average expression. LLC, Lewis lung carcinoma; ES, embryonic stem.

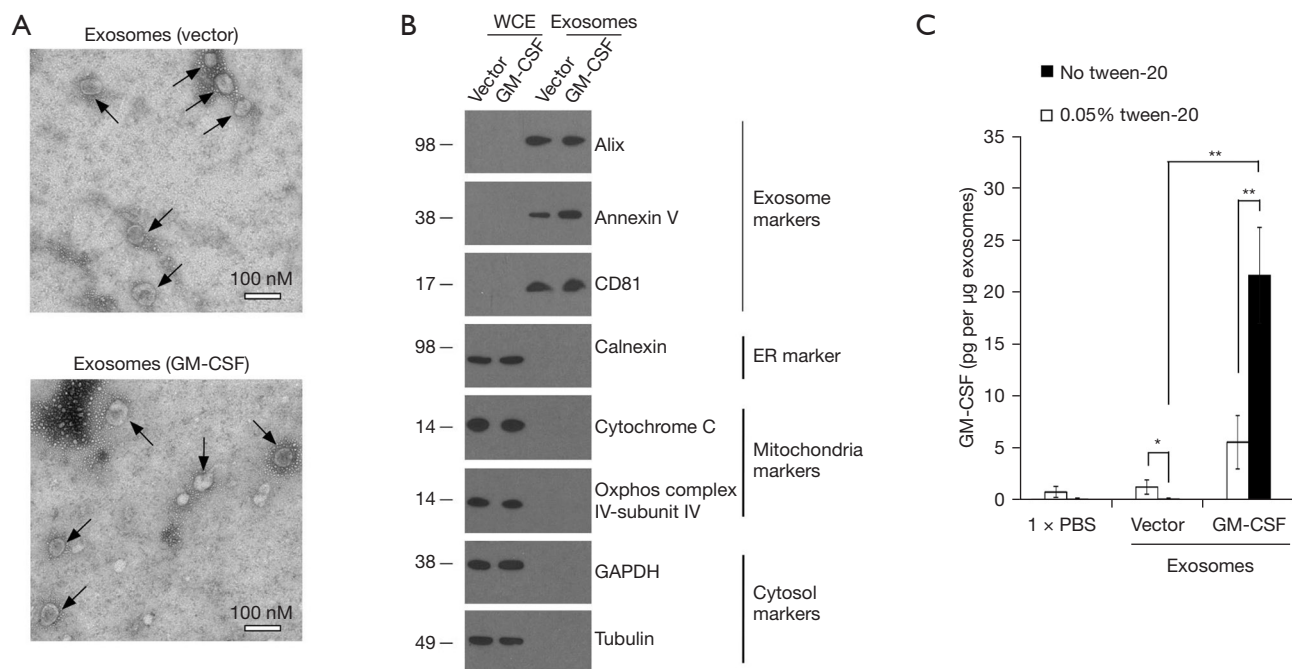


Figure 2 Evaluation of exosomes isolated from ES-D3 cells. (A) TEM images of exosomes acquired from GM-CSF-expressing ES-D3 cells or their vector control counterparts. Scale bar 100 nM. Individual exosomes are indicated by arrows. (B) Western blot evaluation of the indicated markers of exosomes, ER, mitochondria and cytosol in WCE or exosomes. Molecular weights markers (kD) are indicated on the left. (C) The amounts of GM-CSF in the indicated exosomes were measured by ELISA. Exosomes were pretreated with or without 0.05% Tween-20, and ELISA assays were conducted using washing buffer containing either PBS only or PBS + 0.05% Tween-20. The data are presented as mean \pm SD of three independent ELISA measurements. *, $P < 0.05$; **, $P < 0.01$; Unpaired Student's *t* tests. GM-CSF, granulocyte-macrophage colony stimulating factor; WCE, whole cell extracts; ER, endoplasmic reticulum; PBS, phosphate buffered saline; TEM, transmission electron microscopy; SD, standard deviation.

and tubulin (Figure 2B). Next, we evaluated the GM-CSF levels in exosomes by ELISA. We used ELISA to examine the localization of GM-CSF molecules within the isolated

exosomes. We first treated the exosomes with PBS or with PBS/detergent Tween-20 (0.05%); Tween-20 readily permeabilizes the exosomal membrane. ELISA was then

performed in the absence or presence of 0.05% Tween-20. As shown in *Figure 2C*, Tween-20 reduced the background GM-CSF levels in the control exosomes (from 1.24 to 0.057 pg/mg exosomes; $P=0.046$). Conversely, GM-CSF levels in the exosomes acquired from ES-D3 cells expressing GM-CSF were significantly increased in the presence of Tween-20 (from 5.53 to 21.6 pg/mg exosomes; $P=0.0062$). These data indicate that the permeabilization of exosomal membrane by Tween-20 renders intra-exosomal GM-CSF molecules available for antibody detection, suggesting that the majority of exosomal GM-CSF molecules are localized within the isolated exosomes.

Vaccination with ES-exo/GM-CSF inhibits metastasized lung tumor growth

To evaluate the efficacy of ES-exo/GM-CSF vaccine in preventing metastasized lung tumor development, a mouse model of experimental pulmonary metastasis was investigated. In this model, tumor cells injected into the tail vein establish in the lung through blood circulation (21). In this study, C57BL/6 mice were vaccinated at day 0 and again on day 7 with PBS (vehicle control), exosomes from vector control ES-D3 (ES-exo) or GM-CSF-containing exosomes (ES-exo/GM-CSF) via subcutaneous (s.c.) injection (*Figure 3A*). Mice were then challenged with tail vein inoculation of LLC cells (0.15×10^6) at day 14. LLC tumors normally established in the lung around 5 weeks following LLC challenge.

To rigorously examine the vaccination efficacy of ES-exo/GM-CSF on metastasized LLC tumors, we carried out two independent experiments to examine the status of lung tumors at 6 or 7 weeks following initial LLC cell administration. Immediately after collecting lung tissues from the mice in all the experimental groups (indicated above), we first counted the numbers of tumor nodules on lung surface (25). A lung tumor nodule was defined as a discrete, well-defined, rounded opacity that is completely surrounded by lung tissue (*Figure 3B*). Our observations indicate that lungs acquired 6 weeks after LLC inoculation were similar to those obtained 7 weeks post LLC injection (*Figure 3C*). Examination of resected lungs revealed that the numbers of lung tumor nodules in mice vaccinated with ES-exo/GM-CSF were significantly smaller than those in mice injected with vehicle control. The majority of vehicle-administered mouse lungs had surface tumors with an average of 3.5 lesions for each mouse in both 6- and 7-week groups. In contrast, mice vaccinated with ES-exo/GM-CSF

only had an average of 0.4 lesions/mouse (6-week group; $P=0.0099$) or 1.4 lesions/mouse (7-week group; $P=0.0096$), indicating that immunization with ES-exo/GM-CSF inhibited metastatic lung tumor development. The average numbers of tumor nodules in mice vaccinated with ES-exo was higher compared with ES-exo/GM-CSF-immunized mice, but the difference was not significant due to variations among the mice in each group.

To further investigate the efficacy of this vaccination strategy, total lung tumor mass of metastasized LLC was evaluated by a histological approach. Serial sections from each lung resected from the mice were stained with hematoxylin and eosin (H&E) and analyzed by measuring the tumor lesion areas in each lung tissue (*Figure 3D*). Typical lung sections from mice showed a striking difference between PBS-inoculated non-vaccinated mice versus those receiving ES-exo/GM-CSF vaccination. Numerous large tumor lesions were detected in non-vaccinated control mouse lung sections, whereas vaccinated animals were almost free of any detectable lesions (*Figure 3D*). The tumor burden was calculated as the percentage of lung area occupied by tumor lesions in each slide. As shown in *Figure 3E*, ES-exo/GM-CSF-vaccinated mice had a significantly smaller percentage of tumor-bearing lung area compared with the non-vaccinated mice or the mice vaccinated with exosomes without GM-CSF (ES-exo). While average lung tumor burdens of non-vaccinated mice in 6- and 7-week groups were 1.86% and 1.25%, corresponding lung tumor burdens of ES-exo/GM-CSF-vaccinated mice in 6- and 7-week groups were 0.036% ($P=0.0058$) and 0.043% ($P=0.048$), respectively. Absence of metastasized lung tumors in mice immunized with ES-exo/GM-CSF vaccine provides evidence that our vaccination strategy suppresses the development of metastasized lung malignancy, which is in agreement with our earlier studies with subcutaneously implanted LLC tumors (9).

ES-exo/GM-CSF vaccination decreases T_{regs} in lung metastases

To elucidate the underlying mechanisms of the immunity against metastasized lung cancer by ES-exo/GM-CSF vaccination, we analyzed the phenotypes of tumor-infiltrating immune cells by examining the expression of different immune cell markers. Pan-leukocyte marker CD45 was evaluated to ensure that only CD45⁺ immune cells in tumor infiltrates were examined. We first analyzed the effects of our vaccination strategy on tumor-infiltrating T_c and T_{regs} . As shown in *Figure 4A,4B*, immunization with

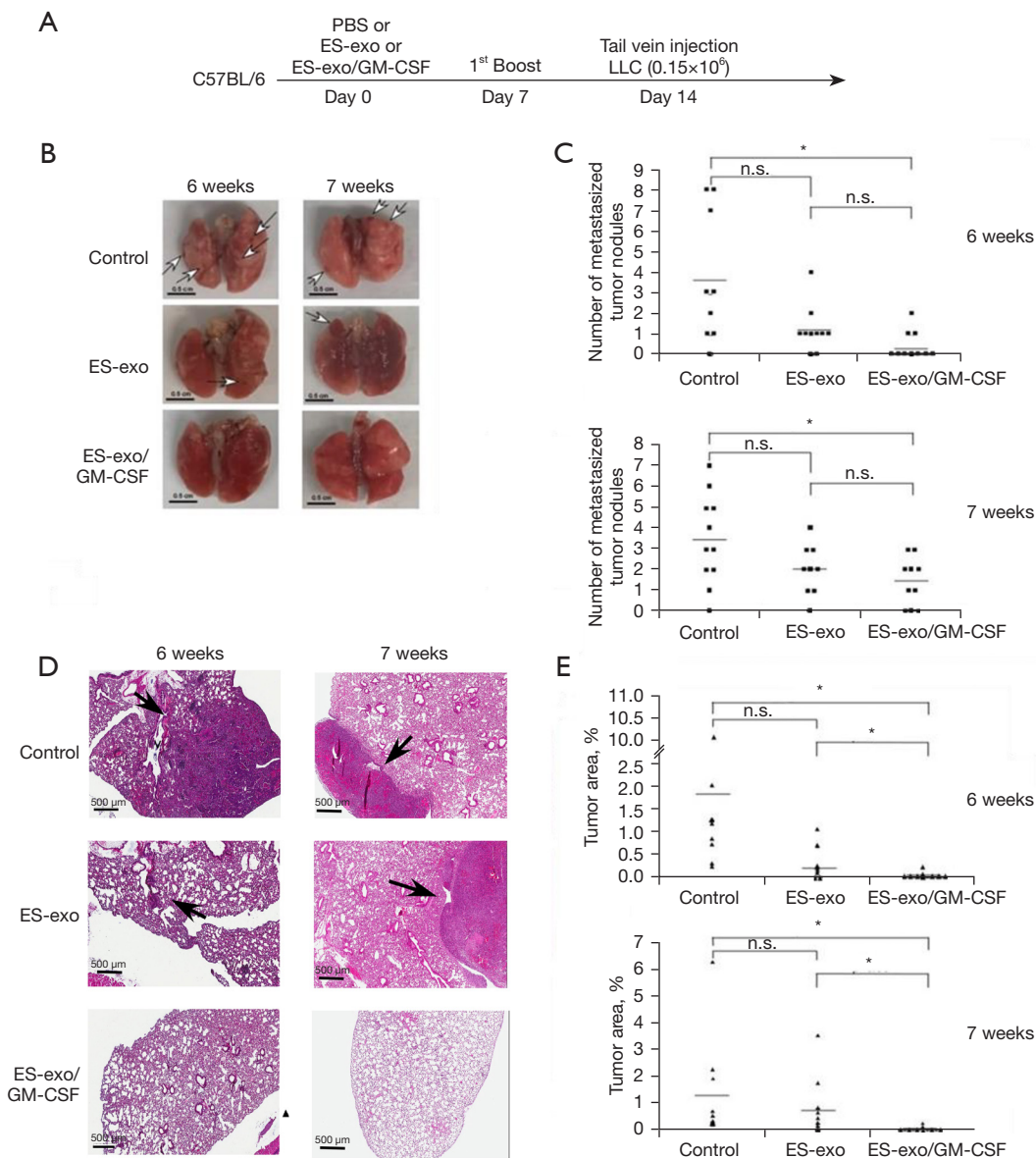


Figure 3 ES-exo/GM-CSF vaccination inhibits the outgrowth of metastatic lung tumors. (A) The scheme of vaccination is depicted. Female C57BL/6 mice were immunized twice (Days 0 and 7) with vehicle control (PBS), ES-exo or ES-exo/GM-CSF prior to tail vein injection with LLC cells (0.15×10^6) on Day 14. Lung tumor development was examined at 6 weeks or at 7 weeks after LLC injection. (B) Representative images of lungs resected from euthanized mice. Surface tumor nodules were indicated by arrows. Scale bar, 0.5 cm. (C) Surface tumor nodules of resected lungs were enumerated by inspection. The data are presented as a dot graph of the number of surface tumor nodules of lungs. In the experiments carried out at 6 weeks after LLC injection, 10 mice in each group were evaluated. In the studies performed at 7 weeks following LLC challenge, $n=11$ mice in control group, $n=9$ mice in ES-exo group and $n=10$ mice in ES-exo/GM-CSF group were examined. *, $P < 0.05$; ANOVA with Tukey's multiple comparison test. (D) The histological sections of resected lungs were examined by H&E staining. Representative images of lung sections are shown (magnification: $\times 200$). Lesions on lung sections are indicated by arrows. Scale bar, 500 μm . (E) The tumor lesion areas of each lung tissue sections were measured. The percentage of total lung area taken up by tumor tissues was quantified via measurements on H&E sections of resected lungs from animals in each group. For each lung, the average value of 3 sections with 50 microns apart was calculated. *, $P < 0.05$; ANOVA with Tukey's multiple comparison test. PBS, phosphate buffered saline; ES, embryonic stem; GM-CSF, granulocyte-macrophage colony stimulating factor; LLC, Lewis lung carcinoma; n.s. not significant; ANOVA, analysis of variance; H&E, hematoxylin and eosin.

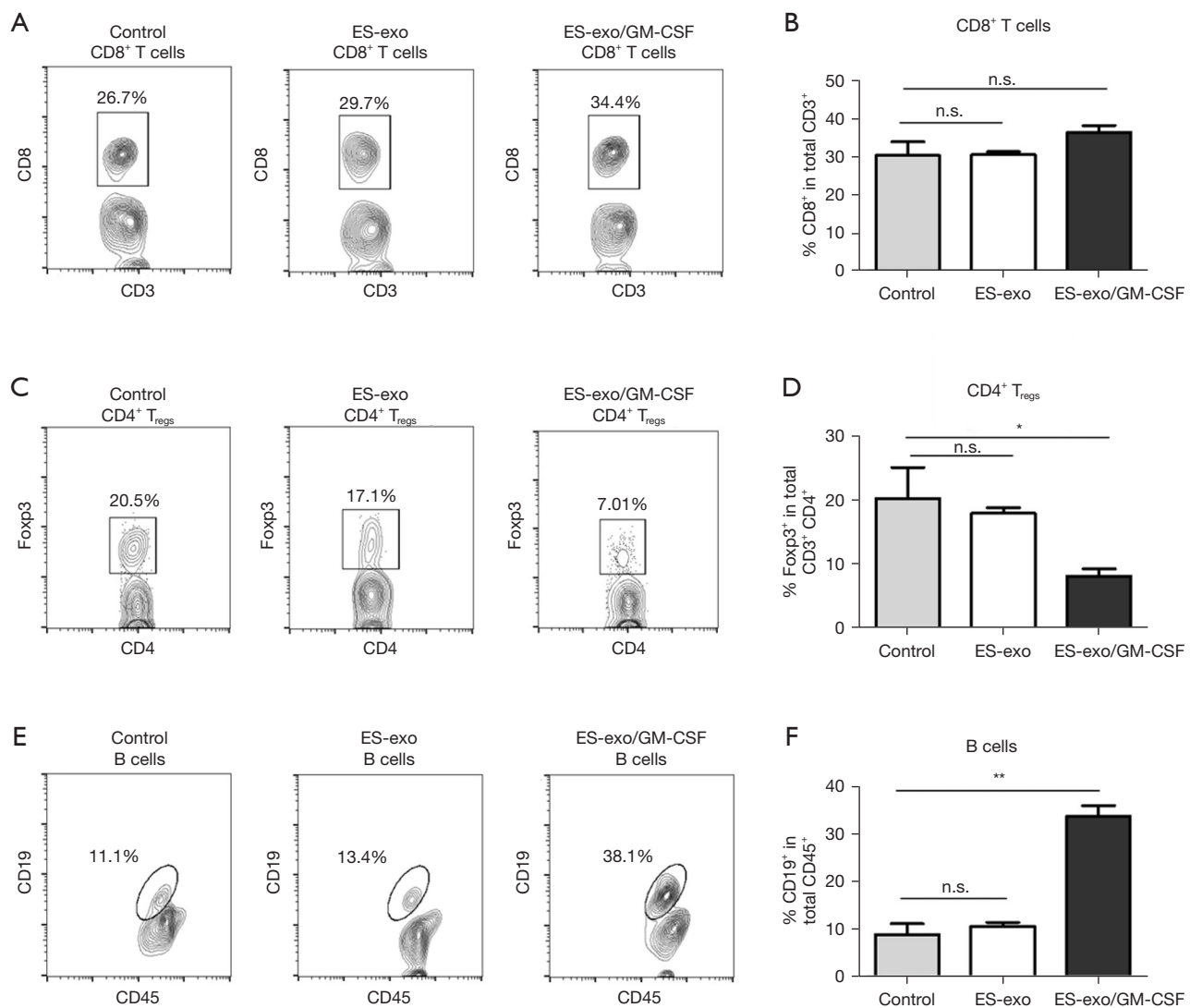


Figure 4 Vaccination of ES-exo/GM-CSF inhibits tumor-infiltrating T_{regs} and increases tumor-infiltrating B cells in metastatic lung tumors. Female C57BL/6 mice were vaccinated twice (days 0 and 7) with PBS (control) or ES-exo or ES-exo/GM-CSF prior to tail vein injection with LLC cells on day 14. Five weeks following LLC challenge, lung tumors were resected, digested by enzymes, and tumor-infiltrating cells were harvested and analyzed by flow cytometry. The pan-hematopoietic marker CD45 was used to identify intratumoral immune cells. (A) The presence of tumor-infiltrating cytotoxic T cells (T_c) was examined and the percentages of $CD8^+$ T_c cells in $CD3^+$ T cell population were determined. (B) Bar graphs showing percentages of tumor-infiltrating $CD8^+$ T_c cells in $CD3^+$ T cells ($n=4$ control and ES-exo group, and $n=6$ mice in ES-exo/GM-CSF group). Mean \pm SD, ANOVA with Tukey's multiple comparison test. (C) Tumor-infiltrating $Foxp3^+$ T_{regs} in $CD3^+$ $CD4^+$ T cells obtained from control, ES-exo and ES-exo/GM-CSF-vaccinated mice were evaluated. Numbers in the plots represent the percentages of subpopulations. (D) Summary of the data shown in (C). $n=4$ in control and ES-exo group, $n=6$ in ES-exo/GM-CSF group; mean \pm SD, *, $P < 0.05$; ANOVA with Tukey's multiple comparison test. (E) Dot plots showing the percentages of $CD19^+$ B cells in $CD45^+$ intratumoral cells obtained from control, ES-exo and ES-exo/GM-CSF-vaccinated mice. Numbers in the dot plots are the percentages of each subpopulation. (F) Bar graphs showing average of percentages of $CD19^+$ B cells in tumor-infiltrating $CD45^+$ cells acquired from control, ES-exo and ES-exo/GM-CSF-vaccinated mice ($n=4$ mice in control and ES-exo group, $n=6$ mice in ES-exo/GM-CSF group). Mean \pm SD, **, $P < 0.01$; ANOVA with Tukey's multiple comparison test. ES, embryonic stem; GM-CSF, granulocyte-macrophage colony stimulating factor; n.s. not significant; PBS, phosphate buffered saline; LLC, Lewis lung carcinoma; SD, standard deviation; ANOVA, analysis of variance.

ES-exo/GM-CSF failed to affect intratumor CD8⁺T_c levels. However, flow cytometry analysis revealed a significant decrease in the percentage of CD4⁺ Foxp3⁺ T_{regs} in the tumor infiltrates from ES-exo/GM-CSF-vaccinated mice when compared with non-vaccinated control mice and ES-exo vaccinated (ES-exo/GM-CSF: 8.16%±1.12%; ES-exo: 18.1%±0.9%; control mice: 20.60%±4.6%; P=0.043, ES-exo/GM-CSF *vs.* control) (Figure 4C,4D).

ES-exo/GM-CSF vaccination promotes intratumoral B cell populations

To explore the effect of ES-exo/GM-CSF vaccination on the levels of B cell populations in metastasized lung tumors, we evaluated the presence of CD19⁺ B cells in intratumoral immune cells. As shown in Figure 4E,4F, the percentage of CD19⁺ B cells in tumor-infiltrating immune cells was significantly increased in mice vaccinated with ES-exo/GM-CSF than their non-vaccinated and ES-exo vaccinated control counterparts (ES-exo/GM-CSF: 33.6%±2.25%; ES-exo: 10.55%±0.86%; control mice: 8.9%±2.20%; P=0.0051, ES-exo/GM-CSF *vs.* control), indicating that vaccination increases B cell levels in tumor infiltrates.

Vaccination with ES-exo/GM-CSF induces anti-tumor cytokine responses

Since cytolytic cytokines produced by tumor-infiltrating CD8⁺ T cells are known to contribute to the anti-tumor function of CD8⁺ T cells (26), we investigated the capability of intratumoral CD8⁺ T cells from vaccinated mice to generate cytokines required for cytotoxic activity against tumors. Tumor-infiltrating immune cells were acquired from metastasized lung tumors in mice immunized with ES-exo/GM-CSF or the vehicle control. Following stimulation with LLC cell lysate, IFN- γ and TNF- α levels in intratumoral CD8⁺ T cells were evaluated. As shown in Figure 5, a significantly higher percentage of IFN- γ -producing CD8⁺ T cells were found in lung metastases in ES-exo/GM-CSF-vaccinated mice and challenged with LLC cells than in their non-vaccinated control counterparts (ES-exo/GM-CSF: 24.70%±0.6%; non-vaccinated control mice: 10.56%±0.9%; P=0.0062). However, the modest increase in TNF- α -producing CD8⁺ T cells promoted by ES-exo/GM-CSF vaccination was not significant (ES-exo/GM-CSF: 79.00%±4.20%; non-vaccinated control mice: 64.55%±4.350%; P=0.1364).

ES-exo/GM-CSF vaccination suppresses tumor-infiltrating myeloid-derived suppressor cells (MDSCs)

In addition to T_{regs}, MDSCs are another prominent suppressor class of innate immune cells hampering anti-tumoral effector responses (27,28). To elucidate the immunomodulatory influences of ES-exo/GM-CSF vaccination, we first evaluated the abundance of CD11b⁺ immune cells in lung metastases. The presence of CD11b⁺ MDSC was significantly reduced from 80.7%±0.2% (control) to 34.9%±2.8% (ES-exo/GM-CSF) (P=0.0018) (Figure 6A,6B). MDSCs are composed of the monocytic subset (M-MDSCs) and granulocytic subset (G-MDSCs), both of which display immune-suppressive capability to promote tumor development (27,28). To further explore the effects of ES-exo/GM-CSF vaccination on intratumoral MDSCs, we examined the presence of MDSC subsets in metastasized lung tumors. As shown in Figure 6C,6D, the percentage of tumor-infiltrating Gr-1⁺ G-MDSCs in CD11b⁺ immune cells was significantly decreased in mice vaccinated with ES-exo/GM-CSF when compared with non-vaccinated and ES-exo vaccinated mice [ES-exo/GM-CSF: 14.9%±0.17%; ES-exo: 66.70%; control mice: 49.5%±2.7%; P=0.0004, ES-exo/GM-CSF *vs.* control]. In contrast, ES-exo/GM-CSF vaccination did not reduce the percentage of Gr-1^{low} M-MDSCs in lung metastases (Figure 6C,6E), suggesting that different subclasses of intratumoral MDSCs play distinct role in anti-tumor efficacy of ES-exo/GM-CSF vaccination.

Vaccination with ES-exo/GM-CSF reduces the percentage of macrophages in metastasized lung tumors

Intratumoral macrophages are associated with initiation as well as progression of various malignancies (29,30). The influence of vaccination with ES-exo/GM-CSF on tumor-infiltrating macrophages was investigated. Previous studies demonstrate that the cell surface protein F4-80 is a major marker of murine macrophages (31). As shown in Figure 6F,6G, the abundance of F4-80⁺Gr-1⁻ macrophages in intratumoral CD11b⁺ myeloid cells was significantly decreased from 15.8% to 3.06% in ES-exo/GM-CSF-vaccinated mice when compared with non-vaccinated and ES-exo vaccinated mice, indicating the involvement of intratumoral macrophages in the immune responses to ES-exo/GM-CSF vaccination (ES-exo/GM-CSF: 4.29%±0.75%; ES-exo: 16.20%±3.4%; control mice: 14.20%±1.6%; P=0.0076, ES-exo/GM-CSF *vs.* control).

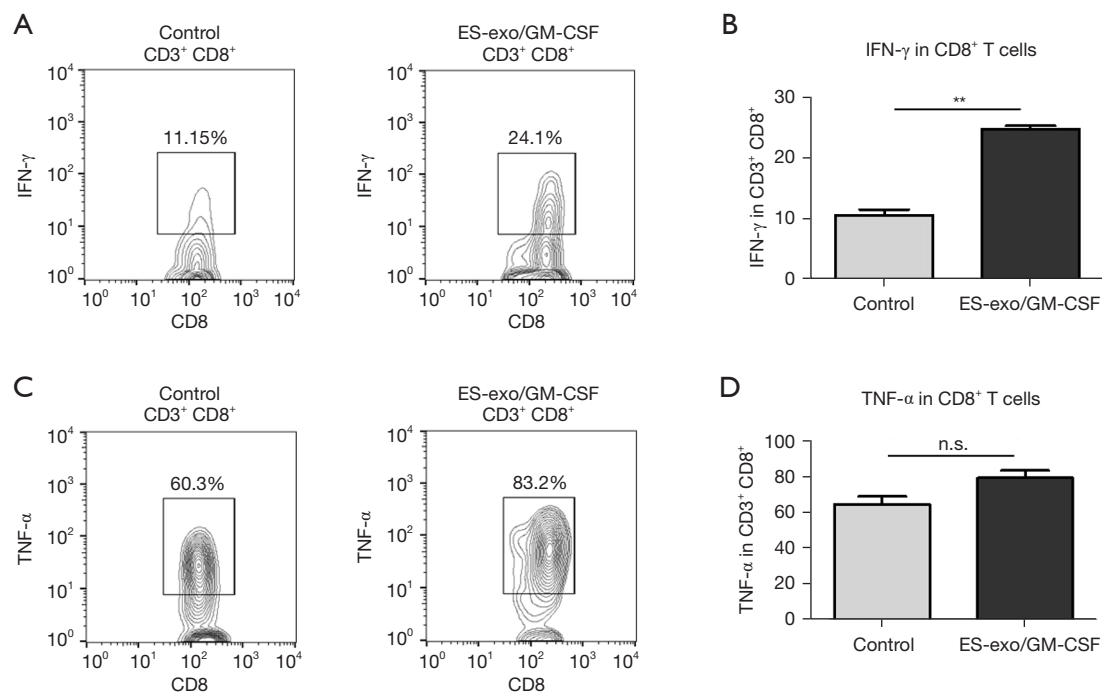


Figure 5 ES-exo/GM-CSF vaccination promotes anti-tumor cytokine production. Female C57BL/6 mice were immunized twice (days 0 and 7) with vehicle control (PBS) or ES-exo/GM-CSF prior to tail vein injection with LLC. Five weeks after LLC challenge, lung tumors were resected, tumor-infiltrating cells were harvested and stimulated with LLC cell lysate for 6 hours. Intratumoral immune cells were identified by the pan-hematopoietic marker CD45 and intracellular expression of IFN- γ and TNF- α was examined by flow cytometry. (A) Dot plots showing IFN- γ expression in tumor-infiltrating CD3⁺CD8⁺ T cells obtained from control and ES-exo/GM-CSF-vaccinated mice. Numbers in plots represent the percentages of each subpopulation. (B) The data shown in (A) are summarized with 4 mice in control group, 6 mice in ES-exo/GM-CSF group. Mean \pm SD, **, $P < 0.01$; ANOVA with Tukey's multiple comparison test. (C) The intracellular expression of TNF- α in tumor-infiltrating CD45⁺CD3⁺CD8⁺ cells was examined by flow cytometry. Numbers indicated in plots are the percentage of each subpopulation. (D) Bar graphs showing average of percentages of TNF- α in intratumoral CD3⁺CD8⁺ T cells from control and ES-exo/GM-CSF-vaccinated mice (n=4 in control group, n=6 in ES-exo/GM-CSF group); mean \pm SD; ANOVA with Tukey's multiple comparison test. ES, embryonic stem; GM-CSF, granulocyte-macrophage colony stimulating factor; n.s. not significant; PBS, phosphate buffered saline; LLC, Lewis lung carcinoma; SD, standard deviation; ANOVA, analysis of variance.

Discussion

The prevalence of pulmonary metastases from different primary tumors is relatively high due to the abundant bloodstream in the lung capillary bed (32). Although there are several therapeutic options available for lung metastases, the overall outcome is still unsatisfactory (16). In this study, we investigated an experimental metastasis model where syngeneic LLC cells were administered directly into the bloodstream of C57BL/6 mice through tail vein injection, primarily resulting in pulmonary metastases (21). We examined the effects of a vaccine composed of exosomes from GM-CSF-expressing ES-D3 cells on lung malignancy. Our data provide evidence that a vaccine derived from GM-

CSF-expressing human ESCs could potentially be used to prevent the development of lung metastases in the future. In our previously published study (9), we had evaluated if any toxicological effects are associated with ES-exo/GM-CSF vaccine treatment in mice bearing implantable tumors. Our published data (9) showed that there were no significant differences in blood cell counts between non-vaccinated, ES-exo and ES-exo/GM-CSF-vaccinated mice. Also, liver and kidney enzymes were unaltered in the vaccinated mice. These studies provided proof that ES-exo/GM-CSF vaccination strategy is safe and does not induce any toxicity in mice. In our study, we have attempted to improve the clinical translatability of our vaccine by employing ES cells engineered to generate GM-CSF. Using these cells, we

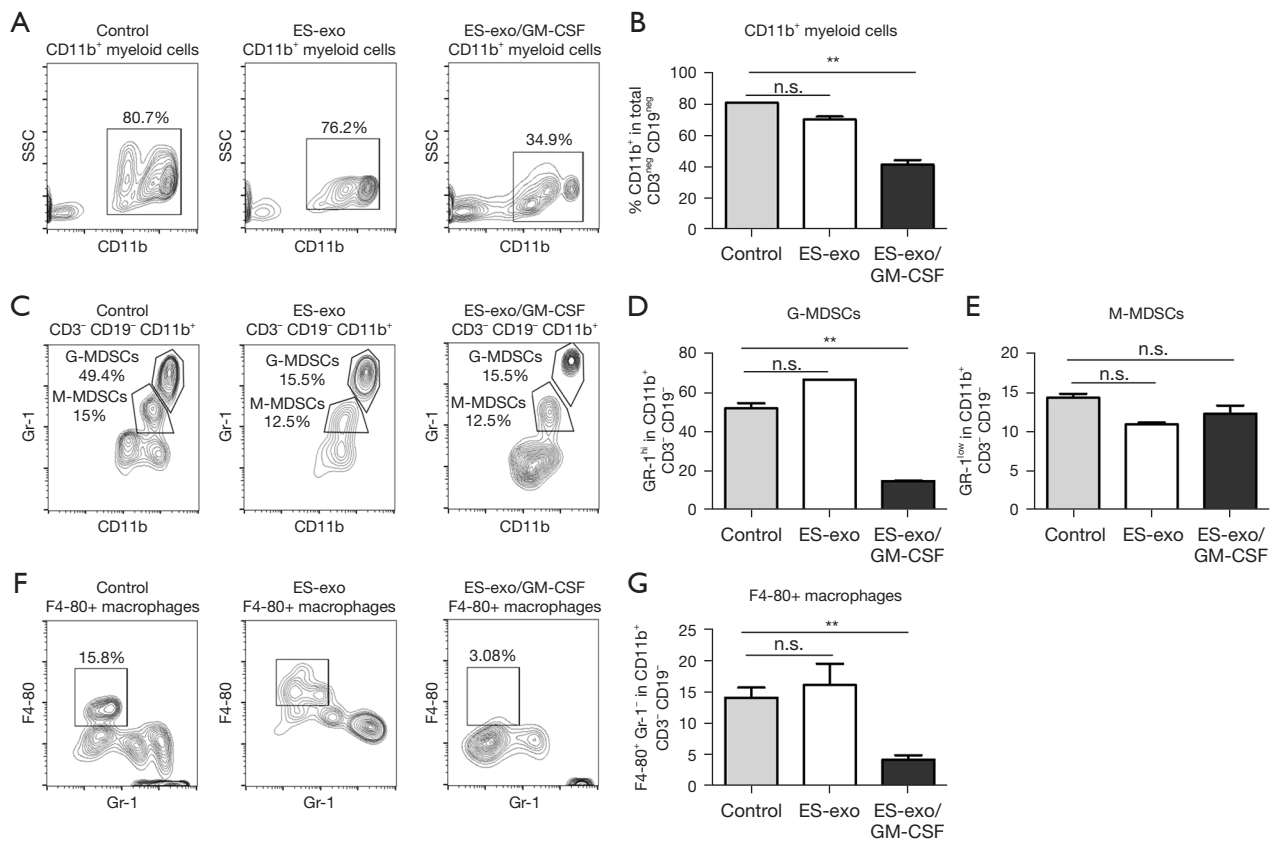


Figure 6 Vaccination of ES-exo/GM-CSF suppresses tumor-infiltrating MDSCs and macrophages. Female C57BL/6 mice were vaccinated with PBS or ES-exo or ES-exo/GM-CSF twice (days 0 and 7) and challenged by tail vein inoculation of LLC cells one week later. MDSCs infiltrating into lung tumors were examined 5 weeks after LLC injection. Intratumoral immune cells were identified by CD45, a pan-hematopoietic marker. (A) Dot plots showing the abundance of CD11b⁺ cells in tumor-infiltrating non-T (CD3⁻) and non-B (CD19⁻) immune cells obtained from control, ES-exo and ES-exo/GM-CSF-vaccinated mice. The percentages of the individual subpopulation are shown. (B) The data shown in (A) are summarized with 4 mice in control and ES-exo group, 6 mice in ES-exo/GM-CSF group. Mean \pm SD, **, $P < 0.01$; ANOVA with Tukey's multiple comparison test. (C) Gr-1^{high} G-MDSCs and Gr-1^{low} M-MDSCs in CD11b⁺ populations shown in (A) were examined. The percentages of each subpopulation are indicated in the graphs. (D,E) Bar graphs show the summarized data presented in (C) (n=4 in control and ES-exo group, n=6 in ES-exo/GM-CSF group); mean \pm SD; **, $P < 0.01$; ANOVA with Tukey's multiple comparison test. (F) The percentages of F4-80⁺GR-1⁻ macrophages in intratumoral non-T (CD3⁻) and non-B (CD19⁻) immune cells from control, ES-exo and ES-exo/GM-CSF-vaccinated mice are shown. Numbers in the plots represent the percentages of each subpopulation. (G) Bar graphs showing the average of percentages of F4-80⁺GR-1⁻ macrophages obtained from control, ES-exo and ES-exo/GM-CSF-vaccinated mice (n=4 in control and ES-exo group, n=6 in ES-exo/GM-CSF group); mean \pm SD; **, $P < 0.01$; ANOVA with Tukey's multiple comparison test. ES, embryonic stem; GM-CSF, granulocyte-macrophage colony stimulating factor; n.s. not significant; MDSC, myeloid derived suppressor cell; PBS, phosphate buffered saline; LLC, Lewis lung carcinoma; SD, standard deviation; ANOVA, analysis of variance; G-MDSC, granulocytic MDSC; M-MDSC, monocytic MDSC.

purified ES-derived exosomes (ES-exo), thereby producing a self-contained, relatively stable exosome-based vaccine. In an experimental metastasis setting, vaccination of mice with ES-exo expressing GM-CSF is effective in preventing implantable lung tumors. Additionally, our observations indicate that administration of recombinant GM-CSF with

intact ES cells is not effective in reducing the lung tumor growth or in inducing anti-tumor immune responses, suggesting a failure of this approach to induce an immune-based suppression of tumor growth. This could be due to the lack of stability of recombinant GM-CSF when injected *in vivo* into mice.

In humans, lung malignancies develop when cancer spreads to lung from where it originates (33). The metastasis mouse model in our study recapitulates the critical process of tumor cell extravasation from blood vessels in target organs, but it lacks the process of tumor cell metastasizing from primary tumor sites and the generation of adhesion and traction forces required for cell migration (21,22). Future research is warranted to investigate the efficacy of ES-exo/GM-CSF in tumor models more truthfully recapitulating the process of metastasis in lung cancer patients.

In our studies, tumor-infiltrating immune cells were acquired from the lungs of vaccinated mice that harbored smaller tumors than those present in non-vaccinated mice (*Figure 3*). The observed difference in intratumoral lymphocyte profiles between vaccinated group and control group could be partially attributed to various stages of lung metastases. More experiments are warranted to examine tumor-infiltrating immune cells from lung metastases at similar stages.

Accumulating evidence indicate that stem-like cells, called cancer stem cells (CSCs) and more differentiated trophoblast-like cells coexist within lung metastases (34,35). With self-renewal and differentiation capabilities similar to those of normal stem cells, CSCs are a likely source of cancer metastases (36). Furthermore, the presence of CSCs is a particular challenge in treating metastasized lung cancer because CSCs tend to be resistant to standard chemotherapy and radiotherapy (37,38). If lung CSCs could be recognized and eliminated by the immune system, the morbidity of cancer metastasis would likely decrease. Earlier studies suggest that the efficacy of ESC vaccination is associated with the immunity targeting CSCs (5). In our study, vaccination with exosomes derived from ESCs induced immune responses against initiation and progression of lung metastases (*Figure 3*). It is conceivable that ES-exo/GM-CSF vaccination triggers immune recognition and eradication of lung CSCs.

Emerging evidence has demonstrated that TILs are deeply involved in metastasis of malignancy (39,40). As ES-exo/GM-CSF vaccination successfully blocked the outgrowth of metastasized lung tumors (*Figure 3*), we evaluated the comprehensive profile of intratumoral immune cells to elucidate the nature of immunity against lung metastases evoked by ES-exo/GM-CSF vaccination. Our study shows that the immune responses induced by exosomes from vector control ES-D3 (ES-exo) were not significantly different from that observed with non-

vaccinated control group (6,9), and accordingly, we did not observe significant changes in the lung tumor growth. In our studies, we found a significant reduction in the presence of T_{regs} in lung metastases of vaccinated/tumor-challenged mice. This is consistent with the findings that increased T_{regs} population in metastasized malignancy often correlates with an immunosuppressive phenotype and poor patient prognosis (41). Similarly, ES-exo/GM-CSF vaccination significantly decreased the abundance of MDSCs, particularly G-MDSC subset, in TILs. As a suppressor of T cell proliferation and activation, MDSCs expansion in TILs is an obstacle in tumor immunotherapy (28). Furthermore, it has been reported that the pulmonary G-MDSC infiltrates are dramatically increased as the metastases form in the lungs to suppress the anti-tumor immune response (42). Therefore, the presence of two prominent suppressor populations that hamper anti-tumoral effector responses, T_{regs} and MDSCs, were suppressed by ES-exo/GM-CSF vaccination, which is correlated with the effectiveness of this vaccine.

$CD8^+$ cytotoxic T cells are known to induce anti-tumor immunity by producing cytolytic cytokines, such as $IFN-\gamma$ and $TNF-\alpha$ (43,44). Cytokines released from tumor-infiltrating $CD8^+$ T cells are crucial contributing factors in immune response against cancer cells (43). ES-exo/GM-CSF vaccination significantly boosted the frequency of $IFN-\gamma$ -producing $CD8^+$ cytotoxic T cells in lung metastases, which is consistent with the data acquired from subcutaneously injected lung tumors (9). However, the levels of $TNF-\alpha$ -producing $CD8^+$ cytotoxic T cells in metastasized pulmonary malignancies were unaffected by ES-exo/GM-CSF vaccination. In contrast, the levels of $TNF-\alpha$ -generating $CD8^+$ cytotoxic T cells in subcutaneously implanted lung tumors were markedly increased by ES-exo/GM-CSF vaccination (9), suggesting that different tumor microenvironments might determine the production of cytokines by $CD8^+$ cytotoxic T cells. Our previous data with implantable tumor models indicate that vaccination with GM-CSF-expressing ESC-derived exosomes induces anti-tumor immune responses in the periphery of the immunized mice (9). Based on this knowledge, it is possible that ES-exo/GM-CSF vaccine-induced immune responses may eradicate the tumor cells in the circulation. We will attempt to assess the effects of vaccination-induced immunity against circulating/or metastasized tumor cells in the future studies. We believe that successful delineation of this mechanism will increase the translatability of our vaccination strategy.

In summary, the protection against metastatic lung cancer afforded by ES-exo/GM-CSF vaccination involves a number of immune response pathways. Future studies will focus on elucidating how this vaccination strategy not only promotes the effector function of the immune system but also suppresses various immune evasion mechanisms. Importantly, a better understanding of the mechanism of action of our vaccination strategy in tumor-bearing animals can expand our studies to the development of a similar preventive strategy based on exosomes derived from human ESCs, potentially leading to clinical trials of human vaccines to protect against lung cancer.

Acknowledgments

We thank Dr. Julia Chariker and Bioinformatics Core of Kentucky IDeA Networks of Biomedical Research Excellence (KY INBRE, P20GM103436) for analyzing RNA-sequencing data. We are grateful for Mr. Arkadiusz Slusarczyk and Electron Microscopy Core of KY INBRE (P20GM103436) for acquiring transmission electron microscope images.

Funding: This work was supported in part by grants from NIH AA018016 (J.W.E.), Commonwealth of Kentucky Research Challenge Trust Fund (J.W.E.), NIH CA106599 and CA175003 (C.L.), DoD Lung Cancer Research Program LC180452 (C.L), NIH CA198249 and NIH/NIGMS P20GM135004 Project Grant (K.Y.), and Free to Breathe Research Grant (K.Y.), NIH T32ES011564 (A.W.). The funders had no role in study design, data collection and analysis, decision to publish, or preparation of the manuscript.

Footnote

Reporting Checklist: The authors have completed the ARRIVE reporting checklist. Available at <https://sci.amegroups.com/article/view/10.21037/sci-2022-030/rc>

Conflicts of Interest: All authors have completed the ICMJE uniform disclosure form (available at <https://sci.amegroups.com/article/view/10.21037/sci-2022-030/coif>). The authors have no conflicts of interest to declare.

Ethical Statement: The authors are accountable for all aspects of the work in ensuring that questions related to the accuracy or integrity of any part of the work are appropriately investigated and resolved. All animal

experiments were performed in accordance with the American Association for the Accreditation of Laboratory Animal Care (AAALC) guidelines and the “Guide for the Care and Use of Laboratory Animals” (Institute of Laboratory Animal Resources, National Research Council, National Academy Press, 1996). The mouse study was approved by the Institutional Animal Care and Use Committee (IACUC) of the University of Louisville (protocol number: 18301).

Open Access Statement: This is an Open Access article distributed in accordance with the Creative Commons Attribution-NonCommercial-NoDerivs 4.0 International License (CC BY-NC-ND 4.0), which permits the non-commercial replication and distribution of the article with the strict proviso that no changes or edits are made and the original work is properly cited (including links to both the formal publication through the relevant DOI and the license). See: <https://creativecommons.org/licenses/by-nc-nd/4.0/>.

References

1. Mellman I, Coukos G, Dranoff G. Cancer immunotherapy comes of age. *Nature* 2011;480:480-9.
2. Brewer BG, Mitchell RA, Harandi A, et al. Embryonic vaccines against cancer: an early history. *Exp Mol Pathol* 2009;86:192-7.
3. Stonehill EH, Bendich A. Retrogenetic expression: the reappearance of embryonal antigens in cancer cells. *Nature* 1970;228:370-2.
4. Hall C, Clarke L, Pal A, et al. A Review of the Role of Carcinoembryonic Antigen in Clinical Practice. *Ann Coloproctol* 2019;35:294-305.
5. Yaddanapudi K, Mitchell RA, Putty K, et al. Vaccination with embryonic stem cells protects against lung cancer: is a broad-spectrum prophylactic vaccine against cancer possible? *PLoS One* 2012;7:e42289.
6. Kooreman NG, Kim Y, de Almeida PE, et al. Autologous iPSC-Based Vaccines Elicit Anti-tumor Responses In Vivo. *Cell Stem Cell* 2018;22:501-513.e7.
7. Ouyang X, Liu Y, Zhou Y, et al. Antitumor effects of iPSC-based cancer vaccine in pancreatic cancer. *Stem Cell Reports* 2021;16:1468-77.
8. Yamanaka S. Pluripotent Stem Cell-Based Cell Therapy-Promise and Challenges. *Cell Stem Cell* 2020;27:523-31.
9. Yaddanapudi K, Meng S, Whitt AG, et al. Exosomes from GM-CSF expressing embryonic stem cells are an effective prophylactic vaccine for cancer prevention.

- Oncoimmunology 2019;8:1561119.
10. Stremersch S, De Smedt SC, Raemdonck K. Therapeutic and diagnostic applications of extracellular vesicles. *J Control Release* 2016;244:167-83.
 11. Sinha D, Roy S, Saha P, et al. Trends in Research on Exosomes in Cancer Progression and Anticancer Therapy. *Cancers (Basel)* 2021;13:326.
 12. Thakur A, Parra DC, Motallebnejad P, et al. Exosomes: Small vesicles with big roles in cancer, vaccine development, and therapeutics. *Bioact Mater* 2022;10:281-94.
 13. Steeg PS. Tumor metastasis: mechanistic insights and clinical challenges. *Nat Med* 2006;12:895-904.
 14. Fares J, Fares MY, Khachfe HH, et al. Molecular principles of metastasis: a hallmark of cancer revisited. *Signal Transduct Target Ther* 2020;5:28.
 15. Gupta GP, Massagué J. Cancer metastasis: building a framework. *Cell* 2006;127:679-95.
 16. Ganesh K, Massagué J. Targeting metastatic cancer. *Nat Med* 2021;27:34-44.
 17. Stella GM, Kolling S, Benvenuti S, et al. Lung-Seeking Metastases. *Cancers (Basel)* 2019;11:1010.
 18. Justilien V, Fields AP. Utility and applications of orthotopic models of human non-small cell lung cancer (NSCLC) for the evaluation of novel and emerging cancer therapeutics. *Curr Protoc Pharmacol* 2013;62:14.27.1-14.27.17.
 19. Cui ZY, Ahn JS, Lee JY, et al. Mouse orthotopic lung cancer model induced by PC14PE6. *Cancer Res Treat* 2006;38:234-9.
 20. Goto H, Yano S, Zhang H, et al. Activity of a new vascular targeting agent, ZD6126, in pulmonary metastases by human lung adenocarcinoma in nude mice. *Cancer Res* 2002;62:3711-5.
 21. Elkin M, Vlodavsky I. Tail vein assay of cancer metastasis. *Curr Protoc Cell Biol* 2001;Chapter 19:19.2.1-7.
 22. Khanna C, Hunter K. Modeling metastasis in vivo. *Carcinogenesis* 2005;26:513-23.
 23. Fischer AH, Jacobson KA, Rose J, et al. Hematoxylin and eosin staining of tissue and cell sections. *CSH Protoc* 2008;2008:pdb.prot4986.
 24. Théry C, Amigorena S, Raposo G, et al. Isolation and characterization of exosomes from cell culture supernatants and biological fluids. *Curr Protoc Cell Biol* 2006;Chapter 3:Unit 3.22.
 25. Meuwissen R, Berns A. Mouse models for human lung cancer. *Genes Dev* 2005;19:643-64.
 26. Maimela NR, Liu S, Zhang Y. Fates of CD8+ T cells in Tumor Microenvironment. *Comput Struct Biotechnol J* 2019;17:1-13.
 27. Condamine T, Ramachandran I, Youn JI, et al. Regulation of tumor metastasis by myeloid-derived suppressor cells. *Annu Rev Med* 2015;66:97-110.
 28. De Cicco P, Ercolano G, Ianaro A. The New Era of Cancer Immunotherapy: Targeting Myeloid-Derived Suppressor Cells to Overcome Immune Evasion. *Front Immunol* 2020;11:1680.
 29. Qian BZ, Pollard JW. Macrophage diversity enhances tumor progression and metastasis. *Cell* 2010;141:39-51.
 30. DeNardo DG, Ruffell B. Macrophages as regulators of tumour immunity and immunotherapy. *Nat Rev Immunol* 2019;19:369-82.
 31. Lin HH, Faunce DE, Stacey M, et al. The macrophage F4/80 receptor is required for the induction of antigen-specific efferent regulatory T cells in peripheral tolerance. *J Exp Med* 2005;201:1615-25.
 32. Chambers AF, Groom AC, MacDonald IC. Dissemination and growth of cancer cells in metastatic sites. *Nat Rev Cancer* 2002;2:563-72.
 33. Popper HH. Progression and metastasis of lung cancer. *Cancer Metastasis Rev* 2016;35:75-91.
 34. Prabavathy D, Swarnalatha Y, Ramadoss N. Lung cancer stem cells-origin, characteristics and therapy. *Stem Cell Investig* 2018;5:6.
 35. Zakaria N, Satar NA, Abu Halim NH, et al. Targeting Lung Cancer Stem Cells: Research and Clinical Impacts. *Front Oncol* 2017;7:80.
 36. Al-Hajj M, Becker MW, Wicha M, et al. Therapeutic implications of cancer stem cells. *Curr Opin Genet Dev* 2004;14:43-7.
 37. Chang JC. Cancer stem cells: Role in tumor growth, recurrence, metastasis, and treatment resistance. *Medicine (Baltimore)* 2016;95:S20-5.
 38. Batlle E, Clevers H. Cancer stem cells revisited. *Nat Med* 2017;23:1124-34.
 39. Man YG, Stojadinovic A, Mason J, et al. Tumor-infiltrating immune cells promoting tumor invasion and metastasis: existing theories. *J Cancer* 2013;4:84-95.
 40. Pajjens ST, Vledder A, de Bruyn M, et al. Tumor-infiltrating lymphocytes in the immunotherapy era. *Cell Mol Immunol* 2021;18:842-59.
 41. Curiel TJ. Regulatory T cells and treatment of cancer. *Curr Opin Immunol* 2008;20:241-6.
 42. Ouzounova M, Lee E, Piranlioglu R, et al. Monocytic and granulocytic myeloid derived suppressor cells differentially regulate spatiotemporal tumour plasticity during metastatic cascade. *Nat Commun* 2017;8:14979.

43. Hodge G, Barnawi J, Jurisevic C, et al. Lung cancer is associated with decreased expression of perforin, granzyme B and interferon (IFN)- γ by infiltrating lung tissue T cells, natural killer (NK) T-like and NK cells. *Clin Exp Immunol* 2014;178:79-85.
44. Raskov H, Orhan A, Christensen JP, et al. Cytotoxic CD8(+) T cells in cancer and cancer immunotherapy. *Br J Cancer* 2021;124:359-67.

doi: 10.21037/sci-2022-030

Cite this article as: Meng S, Whitt AG, Stamp BF, Eaton JW, Li C, Yaddanapudi K. Exosome-based cancer vaccine for prevention of lung cancer. *Stem Cell Investig* 2023;10:2.

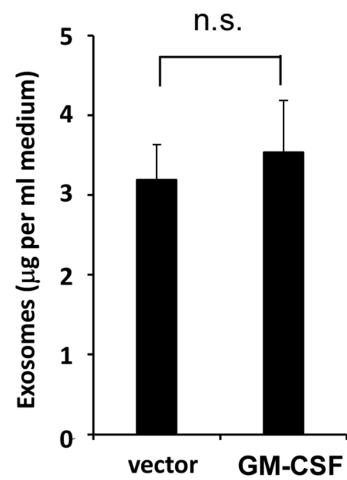


Figure S1 Expression of GM-CSF in ES-D3 cells does not influence the production of exosomes from these cells. Exosomes were acquired from ES-D3 cells expressing the empty vector or GM-CSF. The yield of exosomes was evaluated. The data are presented as mean \pm SD of three independent ELISA experiments. n.s., not significant, Unpaired Student's *t* tests. GM-CSF, granulocyte-macrophage colony stimulating factor; ES, embryonic stem.